Effect of Titania Nanoparticles Loading in Sol-Gel Films for Corrosion Protection of Aluminum AA2024-T3 Alloy in 3.5% Sodium Chloride Solution

Nada F. Atta, Mohamed A. Abd El Fatah, Ahmed Galal[*]

Department of Chemistry, Faculty of Science, Cairo University, 12013 Giza - Egypt
[*]E-mail: galal@sci.cu.edu.eg

Sol-Gel films modified with tiania (TiO_2) was prepared and employed as a corrosion protective coating for aluminum Al2024 (UNS A92024) alloy in 3.5% sodium chloride solution. The morphology of the coatings was analyzed using field-emission scanning electron microscope (FESEM). The protective nature of the coating was evaluated using electrochemical polarization and impedance spectroscopy measurements. The results indicated that the modification of the sol-gel coating with TiO_2 increased the corrosion resistance of the alloy. The insulating and non-permeable nature of the coating resulted in a slower rate of electrolyte penetration to the underlining of the coating. On the other hand, the presence of TiO_2 allowed the modification of the sol-gel structure that ended with a high cross-linked structure. However, we found that increasing the Ti-content allowed high chance for galvanic corrosion that resulted in increasing the corrosion rate. The electrochemical impedance spectroscopy measurements provided an explanation for the increased corrosion resistance of the sol-gel coating containing TiO_2. The surface morphology revealed changes imparted to the surface with and without coating before and after its exposure to the corroding medium.

1. INTRODUCTION

Aluminum and its alloys are an interesting class of materials that have been employed in several applications including aviation, construction and manufacturing [1-3]. AA2024-T3 is among the important alloys of aluminum. Aluminum and its alloys are known to form a passive chemically intact layer of Al_2O_3. The passivity of oxide layer does not hold when exposed to aggressive electrolytes such as sodium chloride. In the latter case, the passive layer is attacked resulting in the

formation of pits [4, 5]. One of the widely used approaches to overcome the oxide layer failure is to coat the surface of the alloy with primers and other coatings [6].

Surface pretreatment of the metallic substrate proved to be effective for achieving better adhesion between the coating layer and the underlying surface [7, 8]. Most organic coatings are hydrophobic in nature and provide barrier-type protection to the substrate [9]. A routine practice protocol depended on the usage of Cr(VI) that results in the formation of a protective oxide over the metal surface [10]. A challenge faced the usage of chromium in industrial application is the leakage of toxic chromium into the environment causing fatal diseases [11]. Other alternatives have been considered for surface pretreatment such as phosphate salts [12], sol-gel techniques [13], silane-based films [14], cerium-impregnated coatings [15, 16] and adsorbed molecular monolayers [17, 18].

Coating layers formed by sol-gel techniques have been used extensively due to the useful properties of the formed films. For instance, sol-gel coatings are conveniently used as "linkers" to bridge the integrity between the metallic substrate and other organic layers anticipated over the alloy surface [19, 20]. Moreover, sol-gel technique allows the addition of well-chosen functional groups that enhance both the mechanical and chemical properties of the resulting protecting films. Sol-gel films can either be formed in aqueous or non-aqueous solvents that improve the properties of the films [21, 22]. Other operational parameters also resulted in fine-tuned film properties. Sol-gel films can be deposited at ambient temperatures and achieve good results without the need of high temperatures needed for the calcination of ceramic type films. Sol-gel films are advantageous over several other types of coatings that realize passive protection for the corroding metallic structure. A disadvantage when using sol-gel films is the formation of defective channels through the layer that results in pores development for electrolytic channeling. Sol-gel layers can be modified by the inclusion of organic inhibitors or nano-structured particles that improve their performance.

The chemical basis of sol-gel film formation is based on hydrolysis/polycondensation reactions of metal alkoxides of the type $[M(OR)_n]$. The rate of reaction decides the nature of the resulting material that range between a sol-like particles to a polymer-like structure in the form of a gel. In recent years, the synthesis of organic–inorganic hybrid coatings attracted a great deal of interest [23, 24]. The inorganic component resulted in enhanced mechanical properties while the organic component leads to increased flexibility and functional compatibility [25].

Different approaches were cited in the literature for inhibiting and protecting AA2024-T3 against corrosion in NaCl containing solutions. Sodium silicate was used with different concentrations in the corroding medium and proved to minimize the corrosion rate of the aluminum alloy [26]. Another study investigated the effect of molar ratio of a coating containing both epoxide and amine functionality [27]. In this study, a self-healing was anticipated to protect the alloy from corrosion. Several inhibitors were also tested including Ce^{3+}, 8-hydroxyquinoline, salicylaldoxime, and 2,5-dimercapto-1,3,4-thiadiazolate when evaluating the corrosion behavior of AA2024-T3 in 0.05 M NaCl [28]. An epoxy coating that contained TiO_2 nanocontainers filled with 8-hydroxyquinoline inhibitor was evaluated for the corrosion protection of the aluminium alloy in 0.05 M NaCl [29]. Sol-gel technique was used to prepare a coating containing two types of silanes, an amino-silane and a sulfur silane for the protection of AA2024-T3 alloy in 3% NaCl [30]. A two-layer coating was used to protect AA2024-T3 made of thin layer of mesoporous silica containing benzotriazole and an acrylic layer [31].

The protection of the aluminium alloy from corrosion in NaCl solution was also achieved by using a sol-gel coating containing cerium nitrate [32].

In this work, we studied the effect of titanium oxide loading in a sol-gel film coating on the corrosion behavior of aluminum alloy AA2024-T3 in 3.5% NaCl solution. It is of prime importance to relate the role played by the titania in enhancing the extent of crosslinking of the sol-gel polymeric film and its effect on the local galvanic corrosion developed during the electrochemical polarization. The morphological structure of the surface before and after exposure to the chloride-containing solution will be also presented.

2. EXPERIMENTAL

2.1 Materials and reagents

AA2024-T3 aluminum alloy was obtained from Alfa Aesar (England) and used as substrate. The nominal composition of the used alloy is given in Table 1 [33].

All chemicals were used without further purification. Hydrochloric acid, sodium chloride, tetraethyl-orthosilicate (TEOS), phenyl-trimethoxysilane (PTEOS), titanium (IV) butoxide, and ethanol were supplied by Sigma-Aldrich Chem. Co. (USA). Aqueous solutions were prepared using double distilled water.

Table 1. Weight percentage composition of AA2024-T3 aluminum alloy

Al	Cu	Cr	Fe	Mg	Mn	Si	Zn	Ti
Bal.	3.8–4.9	<0.1	<0.5	1.2–1.8	0.3–0.9	<0.5	<0.25	<0.15

2.2 Synthesis of sol–gel films and surface casting

The sol gel was prepared by mixing two separate chemicals tetraethyl-orthosilicate (TEOS) and phenyl-trimethoxysilane (PTEOS) and in the presence of dilute HCl as a catalyst, with ethanol as a solvent to give an overall volume of 100 mL. The solution was first mechanically stirred for one hour. From this stock solution, 3 mL volumes were prepared with varying levels of titanium (IV) butoxide to give sols of 0.005 mol L^{-1}, 0.01 mol L^{-1}, 0.05 mol L^{-1}, 0.1 mol L^{-1} and 0.2 mol L^{-1} of titanium-containing sol gel. The resulting solution mixtures were then stirred overnight to bring the reaction to completeness. The prepared AA2024-T3 rods were casted mechanically with the sol, before being spun-coat at up to 1000 rpm and cured for 2 hours at room temperature to form the gel. The resulting films have a final thickness of 1.5 μm (±0.05 μm). The film thickness was determined using an Isoscope® non-destructive coating thickness gauge (Elcome).

The controlled coating technique gave a final thickness of 1.5 μm (±0.05 μm) for all sol–gel coatings, measured using Isoscope® non-destructive coating thickness gauge (Elcome).

2.3 Electrochemical cells and electrode materials

Electrochemical measurements and characterization were carried out with a three-electrode/one compartment glass cell. The working electrode was AA2024-T3 aluminum alloy in the form of a rod of radius ϕ = 0.635 cm. The auxiliary electrode was in the form of 6.0 cm long (0.5 mm thick) platinum wire. All the potentials in the electrochemical studies were referenced to Ag/AgCl (4 mol L^{-1} KCl saturated with AgCl) electrode.

The AA2024-T3 alloy rods with geometrical surface area of 1 cm^2 and protected with a glass tube that was sealed to allow the exposed surface. The alloy surface was mechanically polished with alumina (2 μm)/water-slurry until no visible scratches were observed. Prior to immersion in the cell, the electrode surface was thoroughly rinsed with distilled water and dried. All experiments were performed at 25 °C ± 0.2 °C unless stated otherwise.

2.4 Equipment and experimental set-up

2.4.1 Equipment

Polarization and electrochemical impedance spectroscopy (EIS) measurements were performed using a Gamry-750 instrument and a lock-in-amplifier that are connected to a personal computer.

Scanning Electron Microscope (SEM) were performed using Quanta FEQ 250 (accelerate voltage = 25 kV) 250 instrument to obtain the scanning electron micrographs of the different films. The SEM images were processed with PC connected to the SEM machine.

2.4.2 Experimental set-up

2.4.2.1 Electrodes preparations

The working electrode was thoroughly polished with different grade polishing papers varying from 800-1200 grit size. The electrode was then polished with cloth tissue paper using 1 μm size diamond paste then rinsed with water and sonicated in alcohol/water mixture until a mirror like and scratch-free surface is obtained. For sol-gel coated electrodes; the sol-gel layer and containing the titania with different loading content was deposited as explained earlier in the 2.2 section above.

2.4.2.2. Tafel polarization measurements

The electrodes were subjected to the polarization experiments immediately after polishing. In some experiments the electrodes were left in an "open circuit" setup until a steady state value of the potential is reached showing fluctuations within ± 2 mV. The polarization was performed within the following potential limits E_i = -250 mV and the final potential E_f = +250 mV with respect to open circuit potential and scan rate 5 mV/s for Tafel experiments. For full polarization experiments were

performed within the following potential limits E_i = -1000 mV and the final potential E_f = +1500 mV with respect to open circuit potential and scan rate 1 mVs^{-1}.

2.4.2.3 Electrochemical impedance spectroscopy measurements

The electrochemical impedance spectroscopy (EIS) measurements for the bare, sol gel-coated and Titania-sol gel coated electrodes were performed at room temperature (25 °C ± 0.2 °C) in 3.5% NaCl. The data analysis software was provided with the instrument and applied non-linear least square fitting with Levenberg-Marquardt algorithm. All impedance experiments were recorded between 0.1 Hz and 100 kHz with an excitation signal of 10 mV amplitude. The measurements were performed under potentiostatic control at open circuit potential.

2.4.2.4 Scanning electron microscope (SEM)

Experiments for SEM were performed on the bare and sol gel-containing titania for the coated alloy. Experiments were performed on these samples before and after exposure to the sodium chloride electrolyte. The exposure was achieved by running a Tafel experiment on the samples. In some cases part of the sol gel layer was removed in order to reveal the under laying surface of the alloy. The samples were introduced in the SEM compartment by removing the connecting rod.

3. RESULTS AND DISCUSSION

3.1 Effect of nanoparticles on sol–gel coating

Figure 1 shows the SEM images of the bare AA2024-T3 alloy before (a) and after (b) electrochemical exposure to the corroding 3.5% NaCl medium. As shown in Figure 1(a), the bare alloy has a rough and irregular surface however, after performing Tafel experiment in NaCl medium (Figure 1(b)) pits can be identified on the alloy surface. Figure 1(c) shows the titania sol-gel coated alloy after exposure to the corroding medium (and after partially scratching the surface to reveal the underlying surface), it is clear that pits disappeared. The sol-gel cross linked with titania coating greatly reduces the chance of the electrolyte penetration to the alloy surface (29), which improves the corrosion resistance.

The Tafel polarization curves of bare AA2024-T3 alloy, sol-gel coated and 0.005 mol L^{-1} titania/sol-gel coated alloy in 3.5% NaCl are shown in Figure 2. The electrochemical parameters calculated by Tafel curve fitting are listed in Table 2. Sol-gel coating on AA2024-T3 alloy shows a decrease in corrosion current density (I_{corr}) by about ten time and shift in corrosion potential by about 93 mV towards less noble side of the potential with respect to the bare alloy. The polarization curve of titania sol-gel coated alloy shows shift toward lower current density (about twenty times) and shift in corrosion potential by about 10 mV in noble side of potential compared to the bare alloy. The decrease in corrosion rate in this case can be caused by both the non-permeable nature of the sol-gel coating and

the enhanced structure of the sol-gel by the presence of TiO_2 modifier. This indicates a higher corrosion resistance of the coatings [34, 35]. The protection efficiency can be calculated using the following equation:

$$PE\% = \frac{i^{\circ}_{corr} - i_{corr}}{i^{\circ}_{corr}} \times 100 \qquad (1)$$

Where i°_{corr} is the corrosion current measured at the bare alloy and i_{corr} is the corrosion current measured at the sol-gel coated or sol-gel-titania coated alloy.
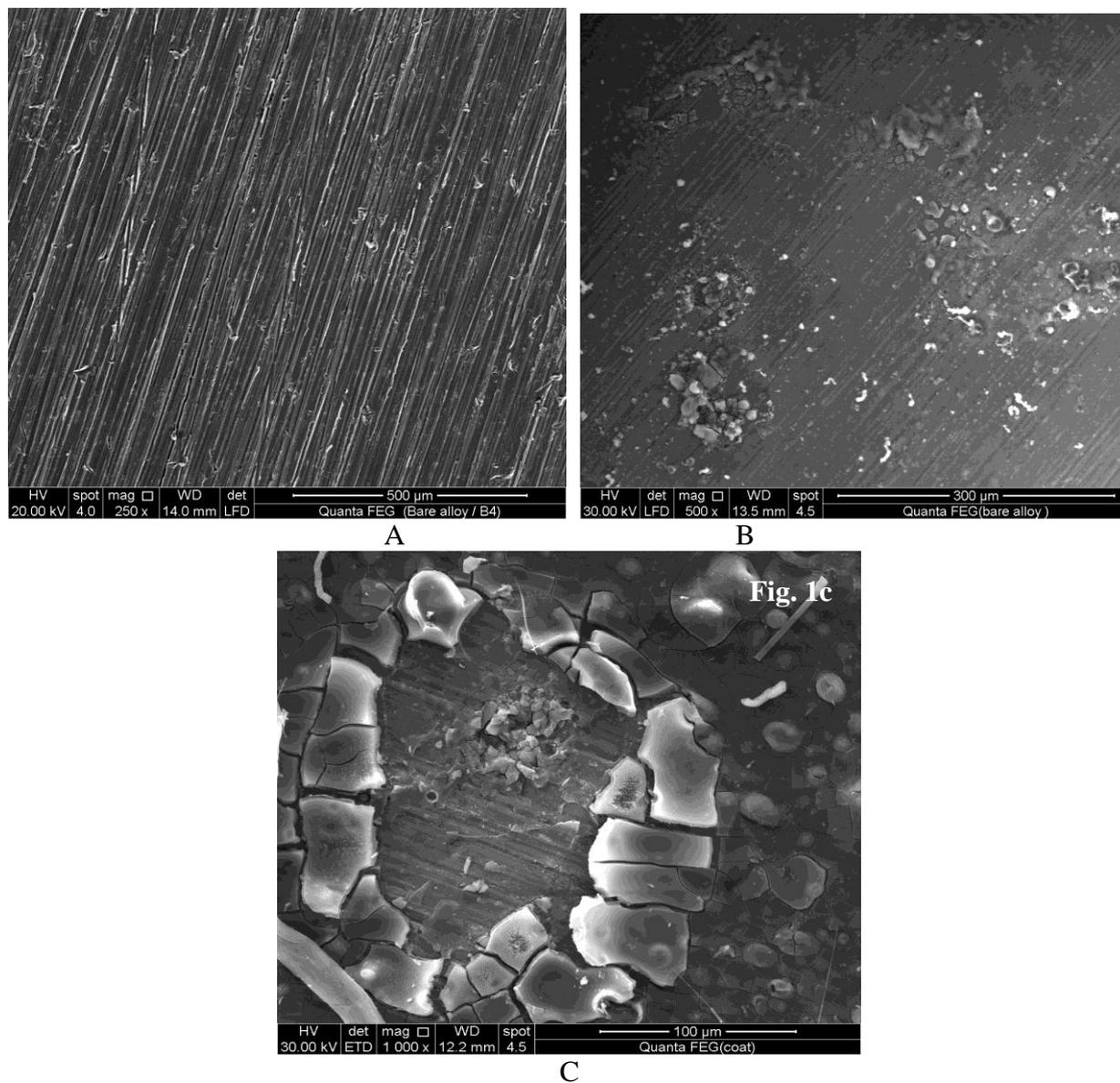

Figure 1. SEM images of the bare AA2024-T3 alloy before (a) and after (b) electrochemical exposure to the corroding 3.5% NaCl medium. (C) Titania sol-gel coated alloy after exposure to the corroding medium (and after partially scratching the surface to reveal the underlying surface)
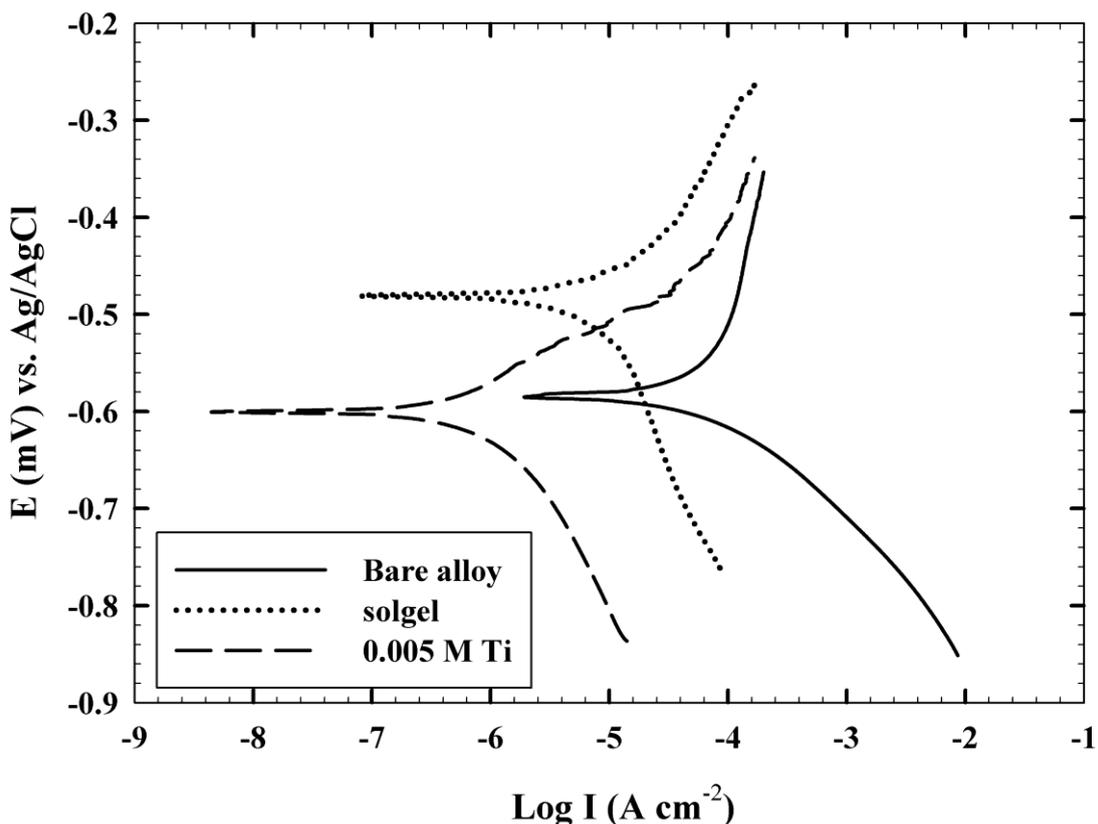
Figure 2. Tafel polarization curves of bare AA2024-T3 alloy, sol-gel coated and 0.005 M titania/sol-gel coated alloy in 3.5% NaCl

Table 2. Electrochemical data of the polarization measurements for bare Al 2024-T3, sol-gel coated electrode, and sol-gel containing different concentrations of titania tested in 3.5% NaCl solution (data from Figures 2 and 5a).

Electrode	I_{corr} (A cm^{-2}) $\times 10^{-6}$	E_{corr} (mV)	β_c (mV decade^{-1})	β_a (mV decade^{-1})	R_p (Ω cm^{-2}) $\times 10^4$	Corr. Rate (mpy)	PE (%)
Bare alloy	128	-584	138	1646	0.0432	1.49	0
Al alloy + sol gel	16.9	-481	514	209	0.382	0.196	86.8
Al alloy + sol gel + 0.005 M TiO$_2$	1.20	-597	204	109	2.92	0.0120	99.1
Al alloy + sol gel + 0.01 M TiO$_2$	1.40	-586	169	63.4	1.38	0.0170	98.9
Al alloy + sol gel + 0.05 M TiO$_2$	3.30	-546	502	124	1.30	0.0390	97.4
Al alloy + sol gel + 0.2 M TiO$_2$	8.80	-557	591	71	0.310	0.0130	93.1

Thus, the sol-gel coating and modification with titania provides protection up to 99.1% in corrosive medium. From the polarization curves, it was found that the coating formed on the aluminum alloy was successful in protecting the surface from corrosion by increasing its electrical resistance [27]. This could be attributed to the degree of cross-linking that varied according to the extent of titania loading in the sol-gel matrix. However, it also shown that the degree of cross-linking is not directly related with the water uptake within the film matrix [27]. Generally all results using different techniques are in good agreement.

The corrosion behavior was also assessed by electrochemical impedance spectroscopy (EIS). The interpretation of impedance spectra was performed after numerical fitting using the general equivalent circuit presented in Figure 3a. In this equivalent circuit, R_{sol} is the solution resistance; R_1 is the pore resistance of the sol–gel/oxide layer interface; Y_{o1} is the surface roughness component of the resistance at the interface; R_{pol} is the polarization resistance due to the charge transfer and C_{dl} is the double-layer capacitance. Figure 3b displays a schematic illustration that describes the matching of circuit elements with the physical structure of the surface. The hybrid film formed possesses high dielectric characteristics. This renders the film electrically resistive and the only possible conduction would be through the pores formed as defects alloying electrolytic diffusion. Similar equivalent circuit was also adopted when examining aluminum alloys coating performance [36]. A previous study showed that the uptake of the electrolyte through the pores of the coating decreases the resistance of the coating and consequently its barrier properties [28].
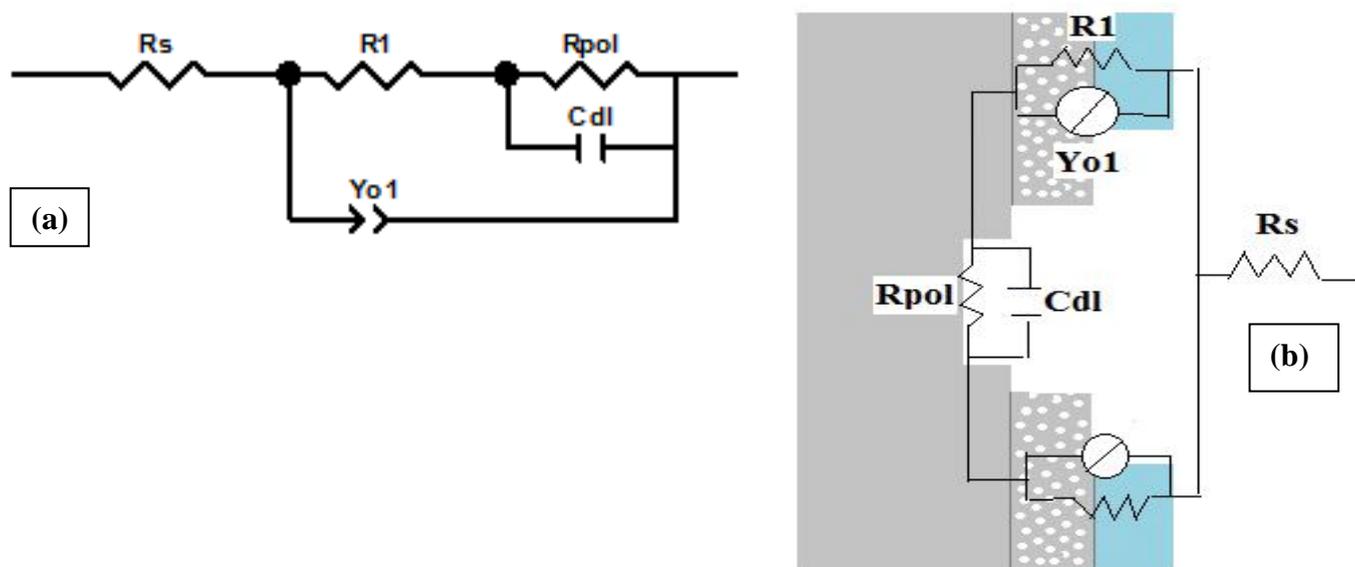

Figure 3. (a) Equivalent circuit used for data fitting of the experimental results of EIS measurements, (b) Physical model of the corrosion processes at the alloy coated with sol gel containing titania nanoparticles.

Figure 4 shows the Nyquist (4a) and Bode (4b) plots obtained for bare AA2024-T3 alloy and titania (0.005 mol L^{-1}) sol-gel coated alloy in 3.5% NaCl solution. As indicated in Table 3, polarization resistance that is a measure of the ease of the charge transfer at the interface of the electrode, increases

noticeably to 9.93×10^3 ohms for the coated electrode compared to 5.27×10^2 ohms of the bare surface. The pore resistance for the coated sample is relatively low (ca. 27 ohm) and did not affect the overall protection ability of the coating.
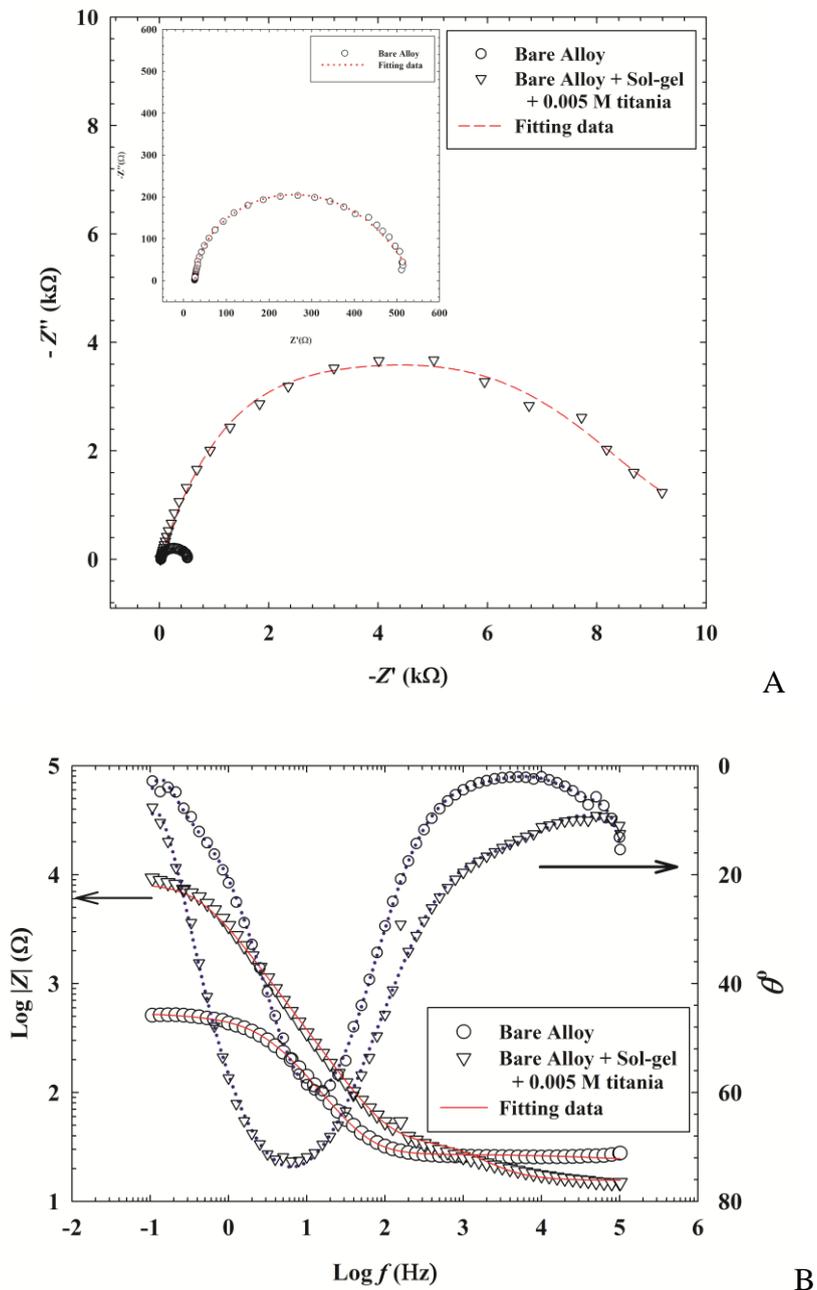

Figure 4. Nyquist (4a) and Bode (4b) plots obtained for bare AA2024-T3 alloy and titania (0.005 mol L^{-1}) sol-gel coated alloy in 3.5% NaCl solution

The quasi-semicircles of Nyquist plots show larger half-diameter for the coated sample compared to the bare surface. A higher phase angle shift of about 79° is also observed at the intermediate frequency range for the coated sample and about 60° for the bare surface. The protection ability for the coating using this hybrid is therefore ascertained. Figure 4B displays two time constants

for the hybrid film over the surface. In the high frequency region (10^5-10^4 Hz), a capacitive behavior is observed representing the sol-gel layer behavior. The lower domain of the frequency at 10-1 Hz describes the formation of an oxide layer that is related to an intermediate interface chemically formed between the aluminum substrate and the Si-containing sol-gel layer. The intermediate frequency region mainly describes the resistive nature of the sol-gel film including the pore defects containing the electrolyte and is represented by a plateau. The data fit of the equivalent circuit are summarized in Table 3.
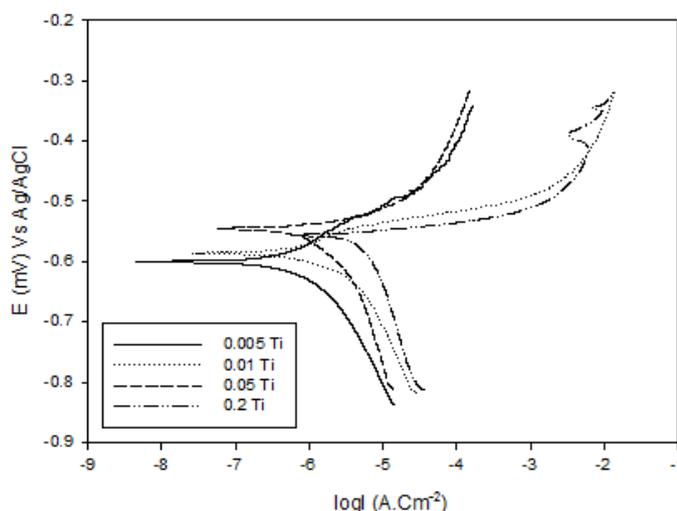
Table 3. Impedance parameters of bare Al2024-T3 alloy and titania (0.005 M) sol-gel coated alloy in 3.5% NaCl solution

Electrode	R_s (Ω cm^2)	R_1 (Ω cm^2)	R_{pol} (Ω cm^2)	Y_{o1} (F cm^{-2} s^n)	n	C_{dl} (F cm^2)	PE (%)
Bare Al6061-T6	20.1	7.24	527	1.89×10^{-4}	0.762	9.87×10^{-5}	--
Sol-gel/0.005 M coated Al2024-T3	15.5	26.1	9930	1.60×10^{-6}	0.895	3.19×10^{-5}	99.3

3.2 Investigation of effect of loaded titania on the coating performance

3.2.1 Effect of molar ratio of titania to sol-gel

The effect of TiO_2 concentration in the sol-gel matrix was also studied by Tafel linear polarization measurements as depicted in Fig. 5a. It can be noticed that changing TiO_2 concentration does not affect the value of corrosion potential. The dependence of the corrosion current, as indicated by the logarithm of current density (A cm^{-2}) at the corrosion potential, on TiO_2 concentration (mol L^{-1}) is given in Fig. 5b.
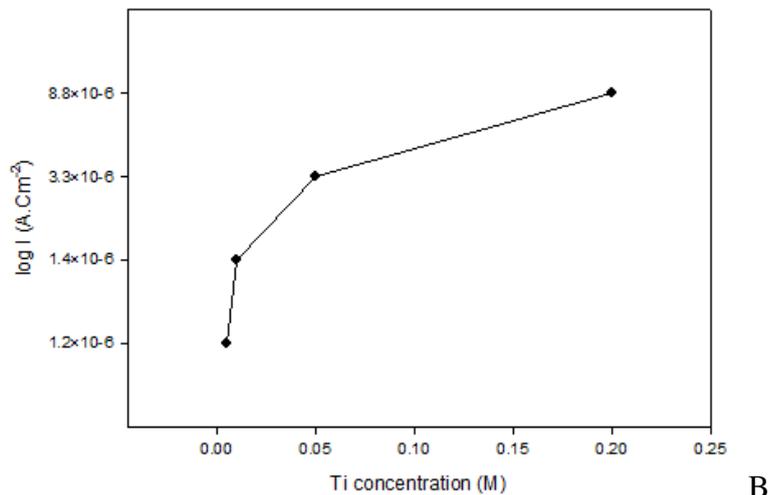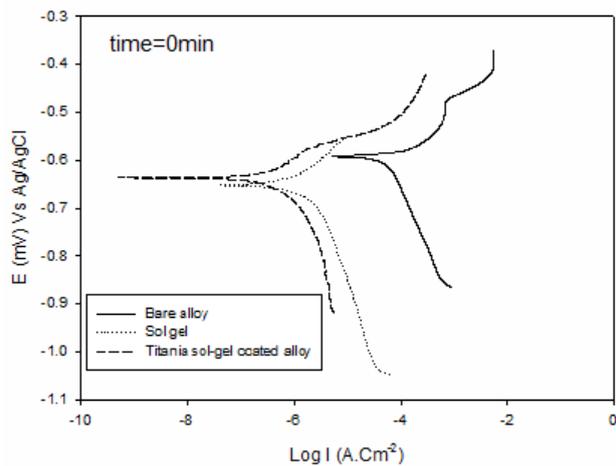
Figure 5. (a) Tafel linear polarization measurements showing the effect of TiO$_2$ concentration in the sol-gel matrix coating over Al2024 in 3.5% NaCl; (b) The dependence of the corrosion current on TiO$_2$ loading in the sol-gel matrix coating (from data of Figure 5(a)).

Relatively lower TiO$_2$ concentrations showed better corrosion resistances than higher concentrations as increasing the TiO$_2$ content allows high chance for galvanic corrosion that resulted in increasing the corrosion rate. Another factor that is the possible increase in pore size of the sol-gel film upon titania incorporation with relatively high concentrations. The typical TiO$_2$ concentration in the sol-gel matrix that results in the lowest corrosion rate is 0.005 mol L^{-1}. As indicated in Table 3, the protection efficiency reaches a maximum when the concentration of TiO$_2$ used is maintained at 0.005 mol L^{-1}. It is important to mention that the protection efficiency calculated from the polarization resistance (of the charge transfer) in the EIS data (Table 3) is comparable to that calculated from the polarization data (Table 2) are comparable. The higher concentration of TiO$_2$ affects the integrity of the sol-gel matrix and allows increasing pore sizes that results in the relative increase in the corrosion current observed.
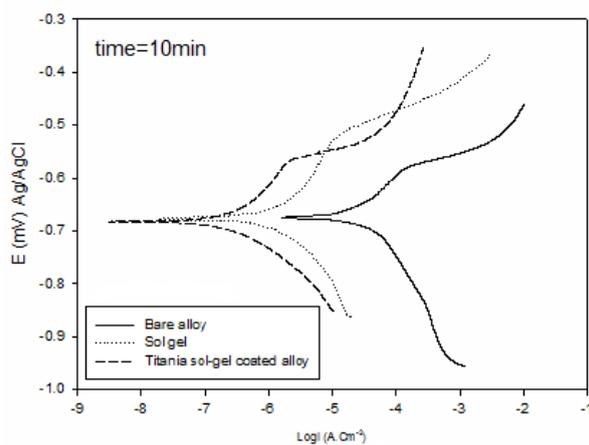
3.2.2 Effect of time of exposure of the alloy to the sodium chloride solution

Figure 6 depicts the polarization curves of coated specimens, with sol-gel and titania sol-gel after 0 minute immersion. It is observed that coated surfaces with titania shows relatively lower corrosion current density and higher polarization resistance compared to that coated with sol-gel.
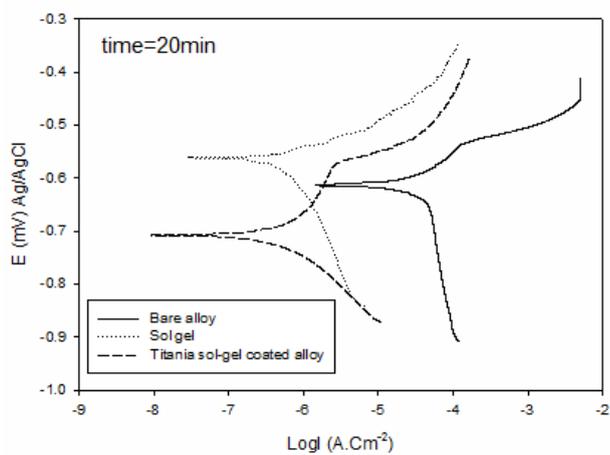
The polarization curves of bare and coated surfaces with sol-gel and titania sol-gel after 0 minute, 10 minutes, 20 minutes, 30 minutes, 60 minutes and 120 minutes immersion are shown in Figures 6a-6f, respectively. The results of all polarization curves for bare and coated AA2024-T3 samples after different immersion times in 3.5% NaCl are given in Table 4. The polarization curves of all coated specimens shift to lower current density values relative to bare alloy. This observation confirms the protection ability of the films against corrosion.
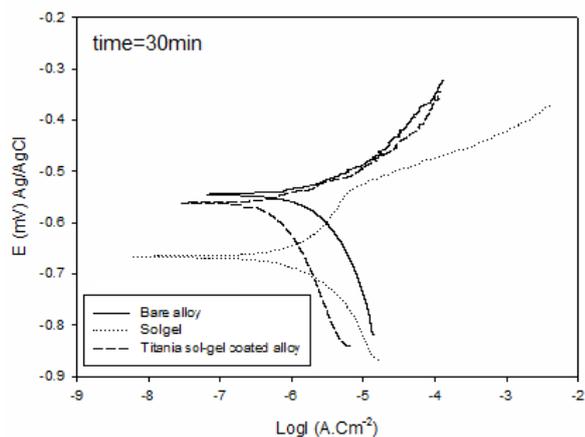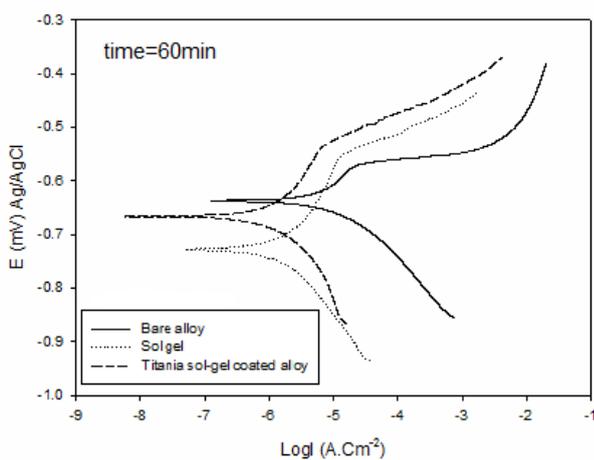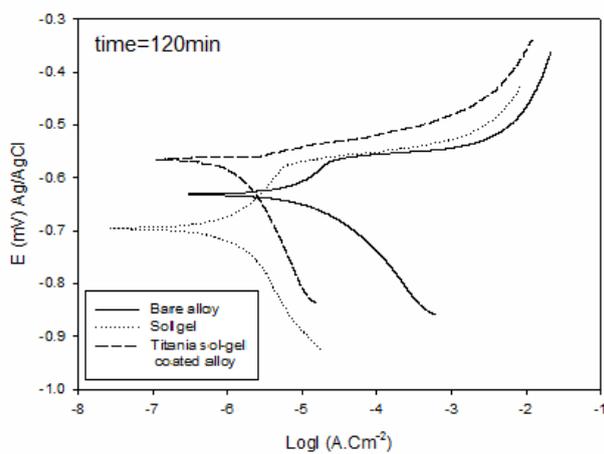
A

B

C

D

E

F

Figure 6. Polarization curves of bare and coated surfaces with sol-gel and titania sol-gel after 0 minute, 10 minutes, 20 minutes, 30 minutes, 60 minutes and 120 (a-f, respectively) minutes immersion in 3.5% NaCl.

Furthermore, the value of i_{corr} for samples coated with titania sol gel is lower than coated alloy specimens with sol gel only. Also, comparison of polarization resistance (R_p) values of coated alloy specimens with sol gel and titania sol-gel improves the corrosion resistance compared to titania-free sol-gel films. It was cited in the literature that the usage of TiO_2 in polymeric epoxy matrices over AA2024-T3 was in the form of nano-containers that enclosed an organic inhibitor [29]. The researchers reported in this work a polarization resistance values in the order of 15.807 kΩ and 24.083 kΩ after 24 h immersion in 0.05 M NaCl for the epoxy coating and epoxy coating containing TiO_2 nano-containers with the organic inhibitor. Incorporation of TiO_2 nanoparticles into the hybrid sols, through hydrolysis and condensation reactions, leads to an additional improvement of the barrier properties due to enhanced thickness and low crack ability of such composites [24, 37]. The overall investigations show that the polarization curves of coated specimens shift slightly to a more negative potential, indicating that difference in the exposed surfaces to the corroding solution.

Table 4. Electrochemical data of polarization curves for bare and sol-gel containing 0.005 M TiO_2 coated AA2024-T3 samples after different immersion times in 3.5% NaCl

Time (min)	Bare alloy			Sol gel-coated electrode			Sol-gel containing 0.005M TiO_2 coated-electrode		
	i_{corr} (A cm^{-2}) $\times 10^{-6}$	E_{corr} (mV)	R_p (Ω cm^{-2})	i_{corr} (A cm^{-2}) $\times 10^{-6}$	E_{corr} (mV)	R_p (Ω cm^{-2})	i_{corr} (A cm^{-2}) $\times 10^{-6}$	E_{corr} (mV)	R_p (Ω cm^{-2})
0	105	-593	1.219	3.1	-651.7	0.037	0.52	-636.5	0.006
10	24.7	-674	0.287	1.03	-677.5	0.012	0.264	-682.6	0.003
20	38.0	-612.3	0.445	1.14	-561.2	0.013	0.385	-708.2	0.004
30	3.99	-544.8	0.046	1.33	-666.5	0.015	1.1	-561.2	0.013
60	4.59	-637.1	0.053	2.13	-727.9	0.025	1.33	-666.5	0.015
120	6.7	-630.9	0.079	3.33	-607.8	0.022	1.76	-565.7	0.021

3.2.3 Effect of temperature

The corrosion of bare AA2024-T3 alloy and titania sol-gel coated alloy in 3.5% NaCl at different temperatures (20–60°C) was studied using Tafel and linear polarization experiments and the electrochemical data are given in Table 5. The protection efficiency was calculated as previously described [35].

The activation energy of the corrosion reaction in the studied range of temperature was calculated using Arrhenius equation:

$$\ln k = \frac{-E_a}{R}\frac{1}{T} + \ln (A) \tag{2}$$

Where k is the rate (expressed in terms of corrosion current densities), E_a is the apparent activation corrosion energy, T is the absolute temperature, A is the Arrhenius pre-exponential constant and R is the universal gas constant. The activation was determined by plotting the logarithm of the

corrosion current (rate) versus 1/T (Figure 7). The calculated value of E_a for bare alloy is 113.1 J mole[-1] and that for sol-gel titania coated alloy is 312.2 J mole[-1]. These values indicate that increasing physical molecular adsorption for the coating containing inhibitor on the AA2024-T3 alloy surface resulted in a better protecting efficiency as the corrosion process is hindered.

Table 5. Electrochemical data of polarization curves for bare and sol-gel containing 0.005 M TiO_2 coated AA2024-T3 samples in 3.5% NaCl at different temperatures

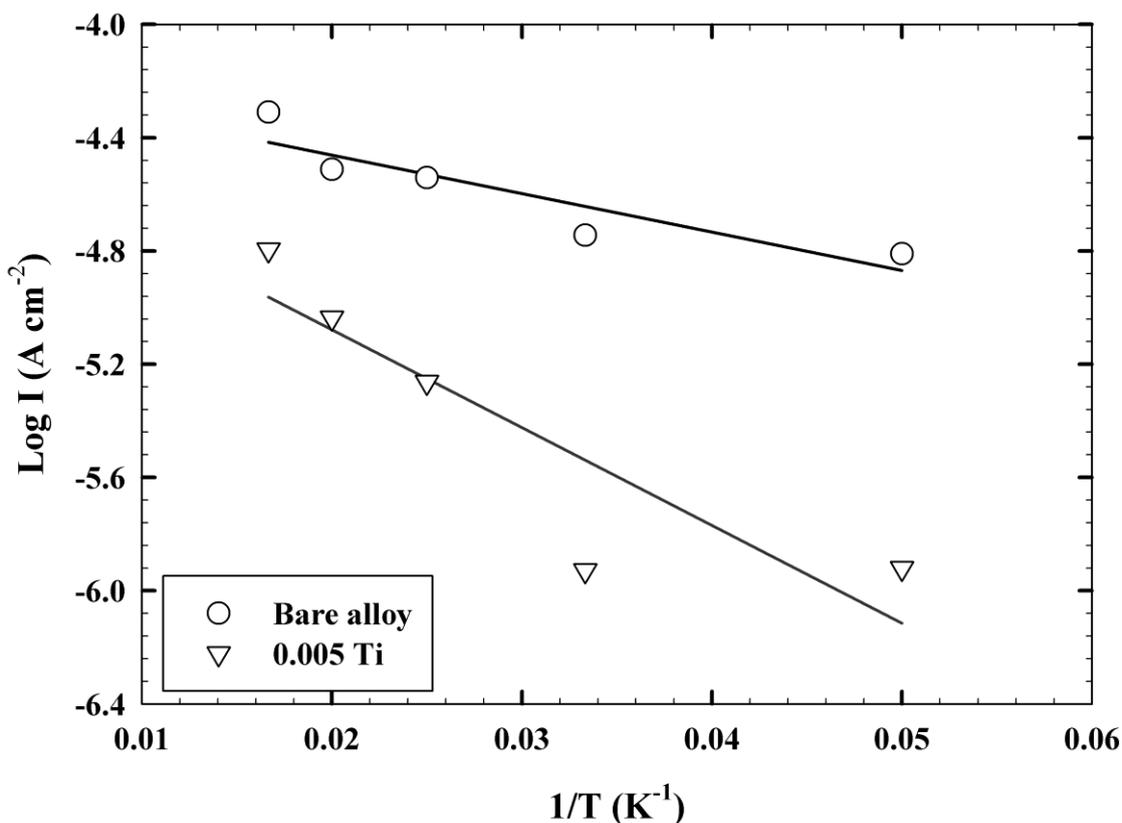| Temperature (°C)	E_{corr} (mV)		I_{corr} (A cm^{-2})		R_p (Ω cm^{-2})		Corrossion Rate (mpy)	
	Bare alloy	0.005 M TiO_2	Bare alloy	0.005 M TiO_2	Bare alloy	0.005 M TiO_2	Bare alloy	0.005 M TiO_2
20	-570.9	-526.7	1.55×10^{-5}	1.2×10^{-6}	1.9×10^3	2.9×10^4	0.18	0.012
30	-574.2	-595.8	1.8×10^{-5}	1.18×10^{-6}	1.7×10^3	1.6×10^4	0.211	0.014
40	-577.1	-625.2	2.88×10^{-5}	5.45×10^{-6}	1×10^3	8×10^3	0.335	0.063
50	-585.3	-588.6	3.08×10^{-5}	9.2×10^{-6}	9.8×10^2	2.7×10^3	0.358	0.108
60	-599.3	-601	4.9×10^{-5}	1.6×10^{-5}	6.9×10^2	1.1×10^3	0.574	0.19

Figure 7. Arrhenius plots of corrosion currents of bare and titania-containing sol gel coatings at different temperatures for AA2024-T3 alloy in 3.5% NaCl

4. CONCLUSIONS

Titania sol-gel coating was successfully employed on AA2024-T3 alloy as an anticorrosive coating. The presence of Ti in the sol-gel affects strongly the anticorrosive performance of the coating as it allows the modification of the sol-gel structure that ended with a high cross-link structure. However, increasing the Ti content allows high chance for galvanic corrosion that resulted in increasing the corrosion rate. The coating proved effective when the coated electrode was tested at temperature as high as 60 °C. The protection efficiency was ascertained from the potentiodynamic and electrochemical impedance measurement. SEM images showed that the surface did not develop pit-formation due to exposure to the NaCl solution.

References

1. A. Yabuki, W. Urushihara, J. Kinugasa and K. Sugano, *Mater. Corros.*, 62 (2011) 907.
2. H. Wang, R. Akid, *Corros. Sci.,* 49 (2007) 4491.
3. M. C. Reboul, B. Baroux, *Mater. Corros.*, 62 (2011) 215.
4. C. F.Malfatti, T. L.Menezes, C. Radtke, J. Esteban, F. Ansart and J. P. Bonino, *Mater. Corros.*, 63 (2012) 819.
5. D. Wang, G. P. Bierwagen, *Prog. Org. Coat.*, 64 (2009) 327.
6. D. Jones, Principles and Prevention of Corrosion, 2nd ed., Prentice Hall Inc., NJ,1996.
7. G.W. Critchlow and D.M. Brewis, *Int. J. Adhes. Adhes.* 16 (1996) 255.
8. G.W. Critchlow, K.A. Yendall, D. Bahrani, A. Quinn and F. Andrews, *Int. J. Adhes. Adhes*. 26 (2006) 419.
9. J.H. Osborne, *Prog. Org. Coat.,* 41 (2001) 280.
10. J. Zhao, L. Xia, A. Sehgal, D. Lu, R.L. McCreery and G.S. Frankel, *Surf. Coat. Technol.*, 140 (2001) 51.
11. R. L. Twite and G. P. Bierwagen, *Prog. Org. Coat.*, 33 (1998) 91.
12. V. Palanivel, D. Zhu and W. J. Van Ooij, *Prog. Org. Coat.*, 47 (2003) 384.
13. N. N. Voevodin, N. T. Grebash, W. S. Soto, L. S. Kasten, J. T. Grant, F. E. Arnold and M. S. Donley, *Prog. Org. Coat.*, 41 (2001) 287.
14. W. Trabelsi, L. Dhouibi, E. Triki, M. G. S. Ferreira and M. F. Montemor, *Surf. Coat. Technol.*, 192 (2005) 284.
15. M. Dabala, E. Ramous and M. Magrini, *Mater. Corros.*, 55 (2004) 381.
16. P. Campestrini, E. P. M. Van Westing, J. H. W. de Wit, *Electrochim. Acta.* 46 (2001) 2631.
17. S. de Souza, D. S. Yoshikawa, W. A. S. Izaltino, S. L. Assis, I. Costa, *Mater. Corros.*, 62 (2011) 913.
18. F. M. Reis, H. G. de Melo and I. Costa, *Electrochim. Acta,* 51 (2006) 1780.
19. M. L. Zheludkevich, I. M. Salvado and M. G. S. Ferreira, *J. Mater. Chem.*, 15 (2005) 5099.
20. N. Voevodin, C. Jeffcoate, L. Simon, M. Khobaib and M. Donley, *Surf. Coat. Technol.*, 140 (2001) 29.
21. A. Atkinson and D. L. Segal, *J. Sol–Gel Sci. Technol.*, 13 (1998) 133.
22. C. J. Brinker and G. Scherrer, Sol–Gel Science: The Physics and Chemistry of Sol–Gel Processing, Academic Press, San Diego, CA, 1990.
23. E. Roussi, A. Tsetsekou, D. Tsiourvas and A. Karantonis, *Surf. Coat. Technol.*, 205 (2011) 3235.
24. M. L. Zheludkevich, R. Serra, M. F. Montemor, I.M. Salvado, M. G. S. Ferreira, *Surf. Coat. Technol.,* 200 (2006) 3084.
25. A. J. Atanacio, B. A. Latella, C. J. Barbe and M. V. Swain, *Surf. Coat. Technol.*, 192 (2005) 354.
26. O. Lopez-Garrity and G.S. Frankel, *Electrochim. Acta*, 130 (2014) 9.

27. T. H. Wu, A. Foyet, A. Kodentsov, L. G. J. van der Ven, R. A. T. M. van Benthem and G. de With, *Mater. Chem. Phys.*, 145 (2014) 342.
28. D. Snihirova, S. V. Lamaka, P. Taheri, J. M. C. Mol and M. F. Montemor, *Surf. Coat. Tech.*, 303 (2015) 342.
29. A. C. Balaskas, I. A. Kartsonakis, L.-A. Tziveleka and G. C. Kordas, *Progr. Org. Coat.*, 74 (2012) 418.
30. S. Beraa, T. K. Routb, G. Udayabhanua and R. Narayan, *Progr. Org. Coat.*, 88 (2015) 293.
31. I. Recloux, Y. Gonzalez-Garcia, M.-E. Druart, F. Khelifa, Ph. Dubois, J. M. C. Mol and M.-G. Olivier, *Surf. Coat. Technol.*, 303 (2016) 352.
32. R. V. Lakshmi, G. Yoganandan, A. V. N. Mohan and B. J. Basu, *Surf. Coat. Tech.*, 240 (2014) 353.
33. Alfa Aesar; Product Certificate of Analysis (Product number 52052), England.
34. F. Andreatta, L. Paussa, P. Aldighieri, A. Lanzutti, D. Raps and L. Fedrizzi, *Prog. Org. Coat.*, 69 (2010) 133.
35. R. Twite, S. Balbyshev and G. Bierwagen, Proc. Symp. Environ. Accept. Inh. Coat., Special Publication of the Electrochemical Society, Pennington 1997, p. 202.
36. C. J. E. De Souza, M. M. Pereira and H. S. Mansur, *J. Mater. Sci. Mater. Med.,* 20 (2009) 61.
37. D. Zhu and W. J. van Ooij, *Corr. Sci.*, 45 (2003) 2177.
38. J. Malzbender and G. de With, *Adv. Eng. Mater.*, 4 (2002) 296.